

# 光学学报

## 衍射多焦点人工晶状体的设计与优化

董博<sup>1,2</sup>, 杨迎<sup>1,2</sup>, 薛常喜<sup>1,2\*</sup>

<sup>1</sup>长春理工大学光电工程学院, 吉林 长春 130022;

<sup>2</sup>长春理工大学先进光学设计与制造技术吉林省高校重点实验室, 吉林 长春 130022

**摘要** 衍射光学设计已经成为人工晶状体设计领域的新兴技术。本文首先分析了衍射多焦点人工晶状体的具体设计流程, 提出了联合非球面衍射基底矫正像质的衍射多焦点人工晶状体设计; 其次针对多焦点衍射光学元件相位结构提出并分析了基底参数对衍射效率的影响的数学模型; 最后通过实例对人工晶状体设计中非球面衍射基底的影响作出了优化。结果表明, 设计流程可用于设计高成像质量多焦点人工晶状体, 基底影响模型可用于分析并优化衍射基底参数对衍射效率的影响。

**关键词** 衍射光学; 人工晶状体; 多焦点; 衍射效率

中图分类号 O436 文献标志码 A DOI: 10.3788/AOS230610

### 1 引言

植入人工晶状体(IOL)作为治疗白内障、高度近视最有效的方法<sup>[1]</sup>, 其光学设计成为热点, 随着人们对成像质量的要求不断提高, 衍射光学元件(DOE)因其任意相位分布<sup>[2-5]</sup>、薄型元件<sup>[6]</sup>、特殊色散<sup>[7-9]</sup>等性质被广泛应用于IOL等眼视透镜设计中。

DOE应用于IOL中通常被用于产生两个或者多个焦点<sup>[10]</sup>。Larsson等<sup>[11]</sup>在1992年提出了双焦点衍射IOL的设计思路, 衍射结构通过一个周期内的固定台阶高度变化, 产生了固定的相位延迟, 从而产生两个不同级次处的衍射效率分布, 21世纪初, 双焦点IOL设计逐渐替代了单焦点IOL, 通常相位延迟被设计为0.5, 以产生相等的远近焦点衍射效率分布, 诸如Tecnis ZMB00、At Lisa 801被广泛应用<sup>[12-13]</sup>。但逐渐两个焦点已无法满足人们的日常使用需求, 为了解决不高的中间视力, 多焦点IOL应运而生, Acrysof IQ PanOptix、FineVision HP等多焦点IOL通过两个双焦衍射结构的适当组合, 不同的相位延迟提供了不同的衍射效率分配, 不同的周期半径提供了不同的附加光焦度<sup>[14]</sup>, 取得了良好的实际效果<sup>[15-16]</sup>。此外如Restor SN6AD3、Acri. Lisa 366D等衍射IOL在提供多焦点的基础上引入了非球面<sup>[17]</sup>, 进一步消除了系统球差, 提高了成像质量, 同时多焦点DOE近年联合连续视程<sup>[18]</sup>、宽波段<sup>[19-20]</sup>等功能以期望提供更全面的视觉效果。综上, DOE被广泛地应用于多焦点IOL设计中,

并朝着多元化方向发展, 故针对衍射多焦点IOL的优化设计变得尤为重要。

然而目前对于多焦点IOL的研究大多基于不同衍射结构的叠加, 当人眼处于明亮环境时, 瞳孔处于相对较小的状态, 边缘衍射结构可能不会过多参与成像, 只有中心的衍射结构起到了作用, 同时过渡区域的成像变化和光线在相邻焦点中产生的干涉导致了视觉质量的恶化, 衍射多焦点透镜有可能产生光晕和眩光<sup>[21]</sup>, 不依赖于瞳孔大小的多焦点设计方法成为研究热点<sup>[22]</sup>。同时DOE应用于眼视透镜时, 不同于红外等系统中应用DOE时的平面基底或者小曲率基底, 由于设计空间的限制, DOE在眼视透镜设计中通常都伴随着一个大曲率基底, 以承担更多的光焦度, 且材料较软, 衍射结构大多倾斜并倾向垂直于大曲率基底, 那么此时衍射基底的影响就不能如大多衍射系统中一样可以被忽略<sup>[23-25]</sup>, 并且随着人们对视觉质量的要求不断提高, 作为一种提高像质的方法, 以后的IOL基底设计必然会上倾向于非球面基底设计<sup>[26-27]</sup>, 则基底参数的变化对衍射性能影响的分析与优化可以弥补眼视透镜设计中理论与实际的差距。

综上所述, 本文首先给出多焦点衍射IOL的设计流程, 提出可以通过同周期内的相位变化实现重点优化中距离的高成像质量多焦点成像, 随后针对本文给出的衍射相位结构, 提出了基底参数对衍射性能影响的模型, 并对衍射基底的影响进行了优化。

收稿日期: 2023-03-01; 修回日期: 2023-04-18; 录用日期: 2023-05-05; 网络首发日期: 2023-06-28

基金项目: 吉林省自然科学基金(20220101124JC)

通信作者: \*xcx272479@sina.com

## 2 多焦点IOL设计

DOE通过在每个环带处产生光程差来产生不同的相位分布,在人眼中,DOE通常设计在透镜前表面上,光线从环境中入射进入DOE,每个环带的周期半径以及附加焦距分别为

$$r^2 = 2\lambda j f, \quad (1)$$

$$f_{\text{order}} = \frac{f}{m}, \quad (2)$$

式中: $r$ 为周期半径; $\lambda$ 为设计波长; $j$ 为环带数; $f$ 为环境中光线经过DOE后的焦距; $m$ 为衍射级次; $f_{\text{order}}$ 为任意衍射级次处的焦距,则相位延迟以及相位差可以分别表示为

$$\beta = \frac{n' - n}{\lambda} h, \quad (3)$$

$$\phi = 2\pi \frac{\lambda}{\lambda_{\text{act}}} \beta, \quad (4)$$

式中: $n'$ 为DOE折射率; $n$ 为环境折射率; $h$ 为台阶高度; $\beta$ 为相位延迟; $\phi$ 为相位差; $\lambda_{\text{act}}$ 为实际波长。则透镜透过率函数的傅里叶级数可以根据相位差表示为

$$c_m = \frac{1}{2\lambda f} \int_0^{2\lambda f} \exp\left(-i\phi \frac{r^2}{2\lambda f}\right) \exp\left(i \frac{m\pi r^2}{\lambda f}\right) dr^2. \quad (5)$$

根据式(5),一个周期内的相位分布决定了总体的衍射效率分布,而常规的同周期单个相位分布衍射结构最

多只能实现两个焦点上的高衍射效率成像。Schwiegerling等<sup>[22]</sup>与Zhang等<sup>[28]</sup>聚焦于通过分区域在一个周期内实现多焦点高衍射效率,则任意相位的DOE的透过率傅里叶级数以及衍射效率更一般的形式可以分别表示为

$$c_m = \frac{1}{2\lambda f} \sum_k^{w_{k+1}} \int_{w_k}^{w_{k+1}} \exp\left(-i\phi_k \frac{r^2}{2\lambda f}\right) \exp\left(i \frac{m\pi r^2}{\lambda f}\right) dr^2, k = 1, 2, 3, \dots, q, w_1 = 0, w_q = 1, 0 \leq w_k \leq 1, w_k < w_{k+1}, \quad (6)$$

$$\eta = c_m^* c_m. \quad (7)$$

对于一般的阶梯式衍射结构而言,式(6)中的 $\phi_k = 2\pi \frac{\lambda}{\lambda_{\text{act}}} \beta_k$

衍射效率是傅里叶级数与其共轭的乘积,综合式(6)和式(7)可以发现,区间之间并不是相互独立的,而是受彼此的影响<sup>[22,28]</sup>。以一个两子区间的设计为例,其他设计区间数的设计同理,整体设计过程可以表示为:首先通过式(6)和式(7)可以得到任意区域划分下的衍射效率分布,以区域划分 $w_1=0.58$ 为例,建立了在两个子区域下的相位延迟 $\beta_1, \beta_2$ 与衍射效率之间的关系,如图1(a)和1(b)所示,然后在图中找寻理想的远、中、近衍射效率对应的相位延迟,最后得到如图1(c)所示的衍射结构图。

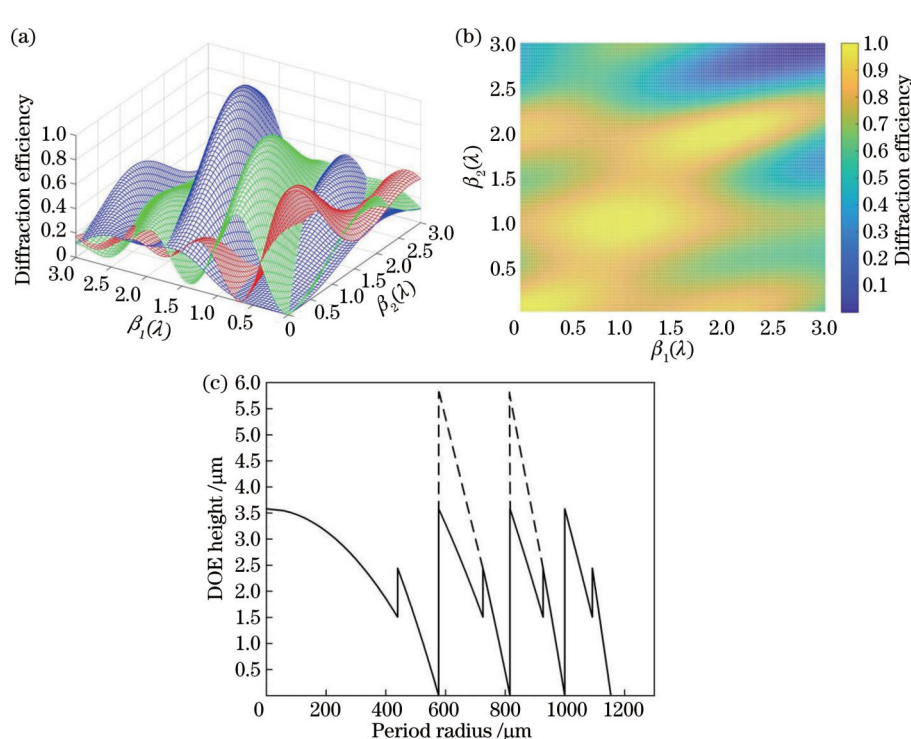


图1 多焦点DOE设计。(a)三个焦点处衍射效率分布(红色: $m=0$ ;绿色: $m=1$ ;蓝色: $m=2$ );(b)总体衍射效率分布;(c)一种分区域DOE台阶高度分布图

Fig. 1 Multifocal diffractive optical element (DOE) design. (a) Diffraction efficiency distributions at three focal points (red:  $m=0$ ; green:  $m=1$ ; blue:  $m=2$ ); (b) overall diffraction efficiency distribution; (c) a step height distribution of sub-region DOE

表1 衍射结构设计参数及结果

Table 1 Design parameters and results of diffraction structure

Parameter	Experimental value
Design wavelength / nm	555
Addition diopters $D$	3.33
Cut-off point $w_1$	0.58
Phase delay $\beta_1(\lambda)$	0.8
Phase delay $\beta_2(\lambda)$	1.3
$m=0:0.2685$	
Result of diffraction efficiency	$m=1:0.3597$
	$m=2:0.2223$

通过选取适当的每个区间的相位延迟,可以实现任意衍射效率分布比例的成像效果<sup>[28]</sup>,针对图1(c)的设计,具体的结构参数与设计结果可见表1,由此得到了一种重点面向中距离的多焦点衍射设计,基于此可通过一个实例来系统化阐述IOL设计的步骤。本文在光学软件中模拟设计了一个三焦点IOL,人眼模型初始结构采用Liou-Brennan人眼模型<sup>[29]</sup>,该模型面向无穷远即视远距离成像,具体参数如表2所示。

表2 Liou-Brennan人眼模型

Table 2 Liou-Brennan human eye model

Surface type	Radius / mm	Thickness / mm	Refractive index	Conic
Standard	7.77	0.50	1.376	-0.18
Standard	6.40	3.16	1.336	-0.60
Standard	Infinity	0	1.336	0
Gradient	12.40	1.59	Grad 1	-0.94
Gradient	Infinity	2.43	Grad 2	0
Standard	-8.10	16.27	1.336	0.96
Standard	-12	—	—	0

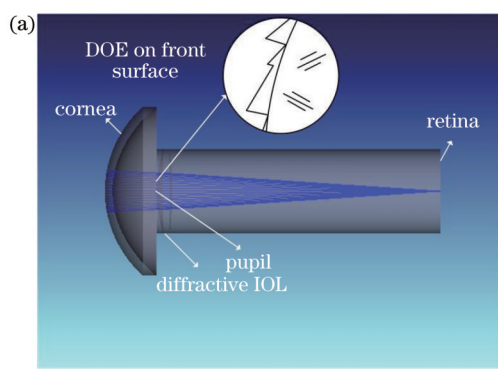


表2中,Grad 1、Grad 2代表渐变折射率<sup>[29]</sup>,在该模型中晶状体承担约18.7D的屈光度,当将模型中的晶状体替换成本文设计的IOL时,IOL屈光度可表示为

$$D = D_{\text{front}} + D_{\text{back}} - \frac{T}{n_{\text{IOL}}} D_{\text{front}} D_{\text{back}}, \quad (8)$$

式中: $D$ 为IOL屈光度; $D_{\text{front}}$ 、 $D_{\text{back}}$ 分别为前后表面屈光度; $T$ 为厚度。通常DOE被设计在前表面上,根据式(1),DOE的加入会带来额外的屈光度即附加光焦度,进一步根据式(2)可以看出,不同衍射级次处提供的屈光度是不同的,在本文设计中DOE最大附加光焦度为3.33D,衍射级次选择 $m=0,1,2$ ,则此时远距离附加光焦度为0,中距离附加光焦度为1.665D,近距离附加光焦度为3.33D。在Zemax中DOE可以用Binary 2面型表示为

$$\phi = m2\pi A_1 r^2, \quad (9)$$

附加光焦度由 $D_{\text{doe}} = -2m\lambda A_1$ 得到。在优化像质时,在Zemax中,DOE被视为一个折射率无穷的薄透镜,Zemax不在乎台阶高度大小或者衍射效率分布,且由表2可计算得到视轴长度为23.95 mm,本文设计的IOL厚度为1.1 mm,可计算得到IOL距视网膜的距离为19.19 mm。则要做到的就是将DOE视为一个薄透镜,在远(对应 $m=0$ )、中(对应 $m=1$ )、近(对应 $m=2$ )三个距离处同时令视网膜处成像质量最佳,优化过程首先将IOL前表面添加圆锥系数与四阶非球面系数,在兼顾IOL基本形状的前提下,继续将IOL后表面设置为非球面,添加圆锥系数与四阶非球面系数,逐步优化,IOL结构参数以及第3节中分析所需要的前表面非球面基底参数在表3中给出,在Zemax中的模拟结构图以及优化后的调制传递函数(MTF)结果在图2中给出。

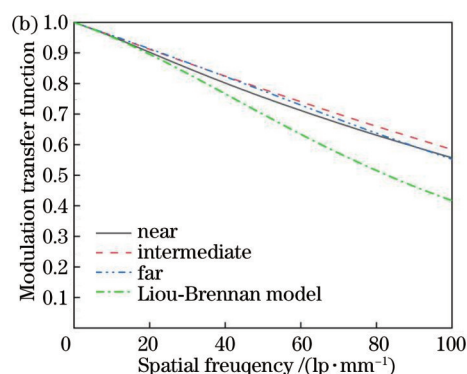


图2 IOL实验仿真图。(a) IOL的3D图;(b) MTF对比图

Fig. 2 Experimental simulation of IOL. (a) 3D image of IOL; (b) MTF comparison

由图2可以看到,在100 lp/mm处近距离MTF为0.5570,中距离MTF为0.5840,远距离MTF为0.5528,超过了Liou-Brennan模型100 lp/mm处的0.3561,在矫正视力的同时优化了人眼成像质量,可以被认定为达到了高成像质量。综上,如图3所示,根据

衍射相位模型完成了对衍射效率分布的研究,并根据在光学软件中的设计完成了对视觉质量的研究,结合两部分设计了一款高成像质量的不依赖瞳孔变化的多焦点IOL,衍射型隐形眼镜、衍射型角膜塑形镜等相关眼视透镜的设计均可参考。

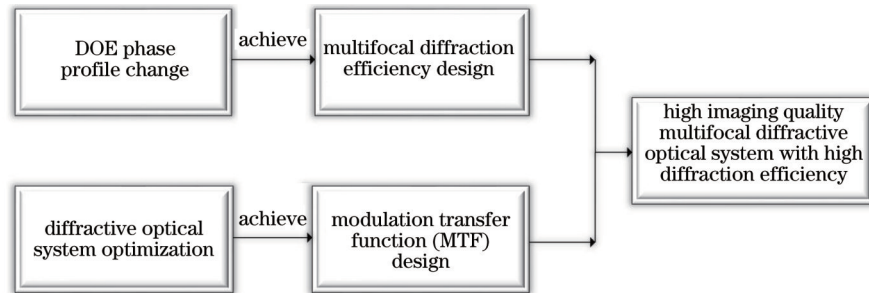


图3 设计流程

Fig. 3 Design process

表3 植入人眼后的IOL设计参数

Table 3 Design parameters of IOL implanted into human eye

Design parameter	Numerical value
Diopters of front surface $D$	13
Thickness /mm	1.1
Semi-diameter /mm	3
Conic of front surface	-5.4545
Fourth-order aspheric coefficient of front surface	$3.6381 \times 10^{-4}$

### 3 衍射基底参数的影响分析与讨论

本节基于第2节给出的多子区域衍射结构设计,分析了衍射基底参数对衍射效率产生的影响。以下过程对双子区域的情况进行分析,任意区域数的分析可类比,但越多的分区域可能给制造带来更大的挑战,需要

设计者权衡。当DOE应用到眼视系统中时,衍射台阶轮廓倾斜并倾向垂直于大曲率基底<sup>[12,30]</sup>,以 $\beta_1$ 小于 $\beta_2$ 的情况为例( $\beta_1$ 大于 $\beta_2$ 时,分析过程可类比推导,不再赘述),此时非球面基底对衍射性能的影响分析如图4所示,其中: $r_{j-1}, r_j$ 分别为第 $j-1$ 、第 $j$ 个周期环带处的衍射周期半径; $z_{j-1}, z_j$ 分别为第 $j-1$ 、第 $j$ 个周期环带截止点处的横向位移。[图5](#)是对图4中相邻衍射周期环带的局部放大图,其中: $h_1$ 为第一个分区域处的台阶高度; $h_2$ 为经过延长后得到的第二个分区域处的台阶高度; $\theta_{d,1}$ 为第一个分区域处的衍射角; $\theta_{d,2}$ 为经过延长后得到的第二个分区域处的衍射角; $\theta_{u,1}, \theta_{v,1}$ 分别为光经过相邻两周期环带时第一个分区域处的光线入射角; $\theta_{u,2}, \theta_{v,2}$ 分别为经过延长后得到的光经过相邻两周期环带时第二个分区域处的光线入射角。则可以得到如下关系式:

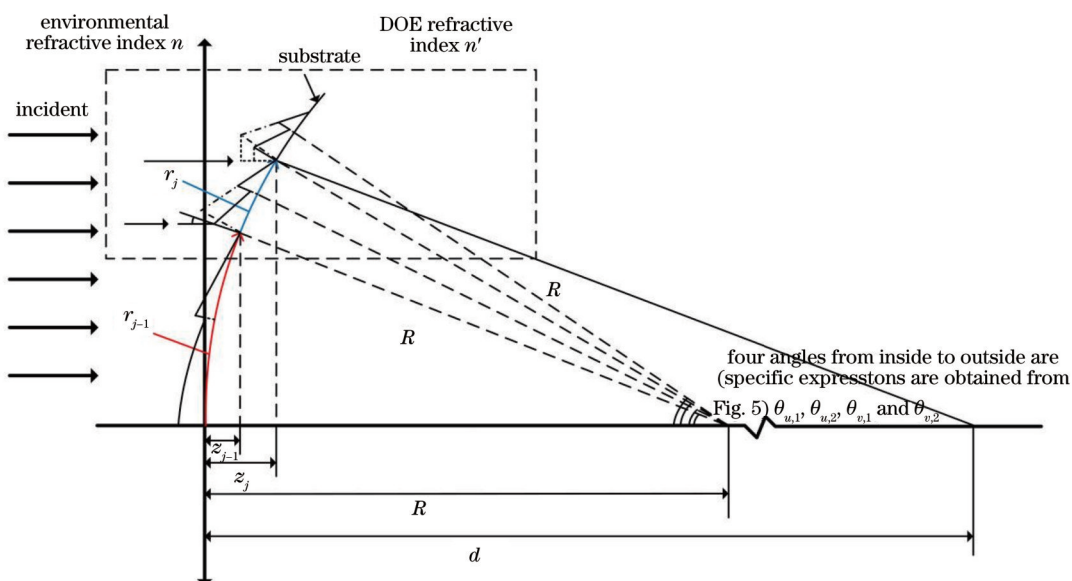


图4 非球面基底对衍射性能的影响分析图

Fig. 4 Analysis of effect of aspheric substrate on diffraction performance

$$n'd - z_j n = n' \sqrt{(d - z_j)^2 + (r_j^2 - z_j^2)} - j\lambda, \quad (10)$$

式中: $d$ 为像距;同时由于 $r_j^2 \gg z_j^2$ ,定义 $a$ 为透镜高度,则 $a^2 \approx r_j^2$ 。在人眼中,99%的像差来自于三阶以及更低阶像差,则用于矫正像质的非球面基底表达式为

$$z_j = \frac{ca^2}{1 + \sqrt{1 - (1 + Q)c^2 a^2}} + Aa^4 = \frac{r_j^2}{2R} + \frac{(1 + Q + 8AR^3)r_j^4}{8R^3}, \quad (11)$$

式中:  $R$  为基底半径;  $Q$  为圆锥系数;  $A$  为四阶非球面系数。定义  $t = Q + 8AR^3$  为非球面综合因子, 结合式(10), 文献[31]中给出了周期半径的表达式为

$$r_j = \sqrt{\frac{2R^2 \left( R - \Delta n f - R \sqrt{\frac{R^3 + n^2 f^2 R + n'^2 f^2 R - 2R^2 f \Delta n - 2Rf^2 n n' - 2\lambda j \Delta n f^2 - 2\lambda j t \Delta n f^2}{R^3}} \right)}{(f \Delta n + f t \Delta n)}}, \quad (12)$$

式中,  $\Delta n = n' - n$ , 则对于分子区域衍射设计, 在图 4~5 中可以得到

$$\begin{cases} l_{u,1} + n'd - nz_{j-1} + (j-1)\beta\lambda = l_{v,1} + n'd - nz_j + j\beta\lambda \\ l_{u,2} + n'd - nz_{j-1} + (j-1)\beta\lambda = l_{v,2} + n'd - nz_j + j\beta\lambda \end{cases}, \quad (13)$$

式中,  $l_{u,1}$ 、 $l_{v,1}$ 、 $l_{u,2}$ 、 $l_{v,2}$  为光程, 由于  $z_{j-1} \approx z_j$ , 则实际的第  $j$  个环带处的相位延迟可以表示为

$$\begin{cases} \beta_{act,j,1} = \frac{l_{u,1} - l_{v,1}}{\lambda} \\ \beta_{act,j,2} = \frac{l_{u,2} - l_{v,2}}{\lambda} \end{cases}. \quad (14)$$

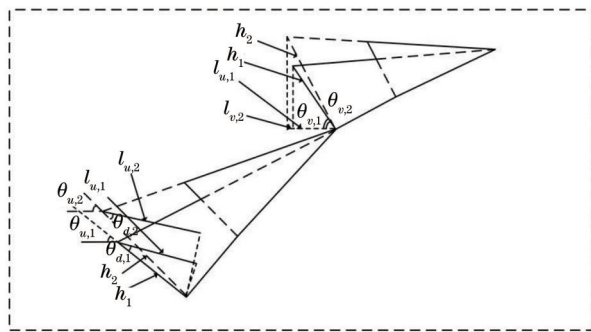


图 5 图 4 的局部放大图

Fig. 5 Partial magnification of Fig. 4

根据 Snell 定律可得相邻两环带的光程为

$$l_{u,reg} = \sqrt{(h_{reg}n')^2 - (h_{reg}n' \sin \theta_{d,reg})^2} = h_{reg} \sqrt{n'^2 - n^2 \sin^2 \theta_{u,reg}}, \quad (15)$$

$$l_{v,reg} = nh_{reg} \cos \theta_{v,reg}, \quad (16)$$

式中,  $reg$  表示所在区间数。对于图 4~5 中的衍射结构, 角度可以通过数学关系表示为

$$\begin{cases} \theta_{u,1} = \frac{r_{j-1}}{R} \\ \theta_{v,1} = \frac{r_j}{R} \end{cases}, \quad (17)$$

$$\begin{cases} \theta_{u,2} = \frac{r_{j-1+w}}{R} \\ \theta_{v,2} = \frac{r_{j+w}}{R} \end{cases}, \quad (18)$$

式中:  $r_{j-1}$ 、 $r_j$ 、 $r_{j-1+w}$ 、 $r_{j+w}$  由式(12)得到;  $w$  即为第一区域所占比例, 得到实际的相位延迟  $\beta_{act,j,1}$ 、 $\beta_{act,j,2}$  的表达式为

$$\begin{cases} \beta_{act,j,1} = \frac{l_{u,1} - l_{v,1}}{\lambda} = \frac{h_1 \sqrt{n'^2 - n^2 \sin^2 \theta_{u,1}} - nh_1 \cos \theta_{v,1}}{\lambda} \\ \beta_{act,j,2} = \frac{l_{u,2} - l_{v,2}}{\lambda} = \frac{h_2 \sqrt{n'^2 - n^2 \sin^2 \theta_{u,2}} - nh_2 \cos \theta_{v,2}}{\lambda} \end{cases}, \quad (19)$$

代入式(6)和式(7)中得到实际的傅里叶展开表达式以及衍射效率表达式分别为

$$c_{m,act,j} = \frac{1}{2\lambda f} \left[ \int_0^{2w_1\lambda f} \exp \left( -\frac{-i2\pi\beta_{act,j,1}r^2}{2\lambda_{act}f} \right) \exp \left( \frac{im\pi r^2}{\lambda f} \right) dr^2 + \int_{2w_1\lambda f}^{2\lambda f} \exp \left( -\frac{-i2\pi\beta_{act,j,2}r^2}{2\lambda_{act}f} \right) \exp \left( \frac{im\pi r^2}{\lambda f} \right) dr^2 \right], \quad (20)$$

$$\eta_{act} = c_{m,act,j}^* c_{m,act,j} \quad (21)$$

首先以常见的 IOL 设计参数为例进行分析, 衍射结构通常设计在 IOL 前表面上, 前表面常见屈光度范围为 0~20D, 非球面综合因子在考虑加入非球面系数后的透镜面型形变因素后, 采用可以包含常规 IOL 设计范畴的 -60 到 60。为方便对比效果, 衍射结构初始参数选取远中近衍射效率分布均匀的参数, 此时  $\beta_1$  为 0.53,  $\beta_2$  为 1.29, 分区域比例为 11:9, 远、中、近衍射效率分别为 0.2698、0.2750、0.2783。由于变化规律是固定的, 中心 3 个衍射环带区域在人眼处于明亮或昏暗环境下时均常被使用, 为应用核心区域, 故接下来的只对中心 3 个衍射环带区域进行分析。

图 6 中构建了周期环带数为 1~3, 衍射级次  $m$  分别为 0、1、2 时, 基底屈光度和非球面综合因子对衍射效率的影响。当没有非球面综合因子加入时, 随着屈光度即曲率的增加, 基底的影响逐渐增大, 即曲率的增加导致实际衍射效率与平面基底衍射效率逐渐偏离, 其中当非球面综合因子为 0, 屈光度为 0 时, 符合平面基底衍射时得到的衍射效率大小; 当非球面综合因子为负数时, 整个基底会由弯曲向着平面发展, 这时总体

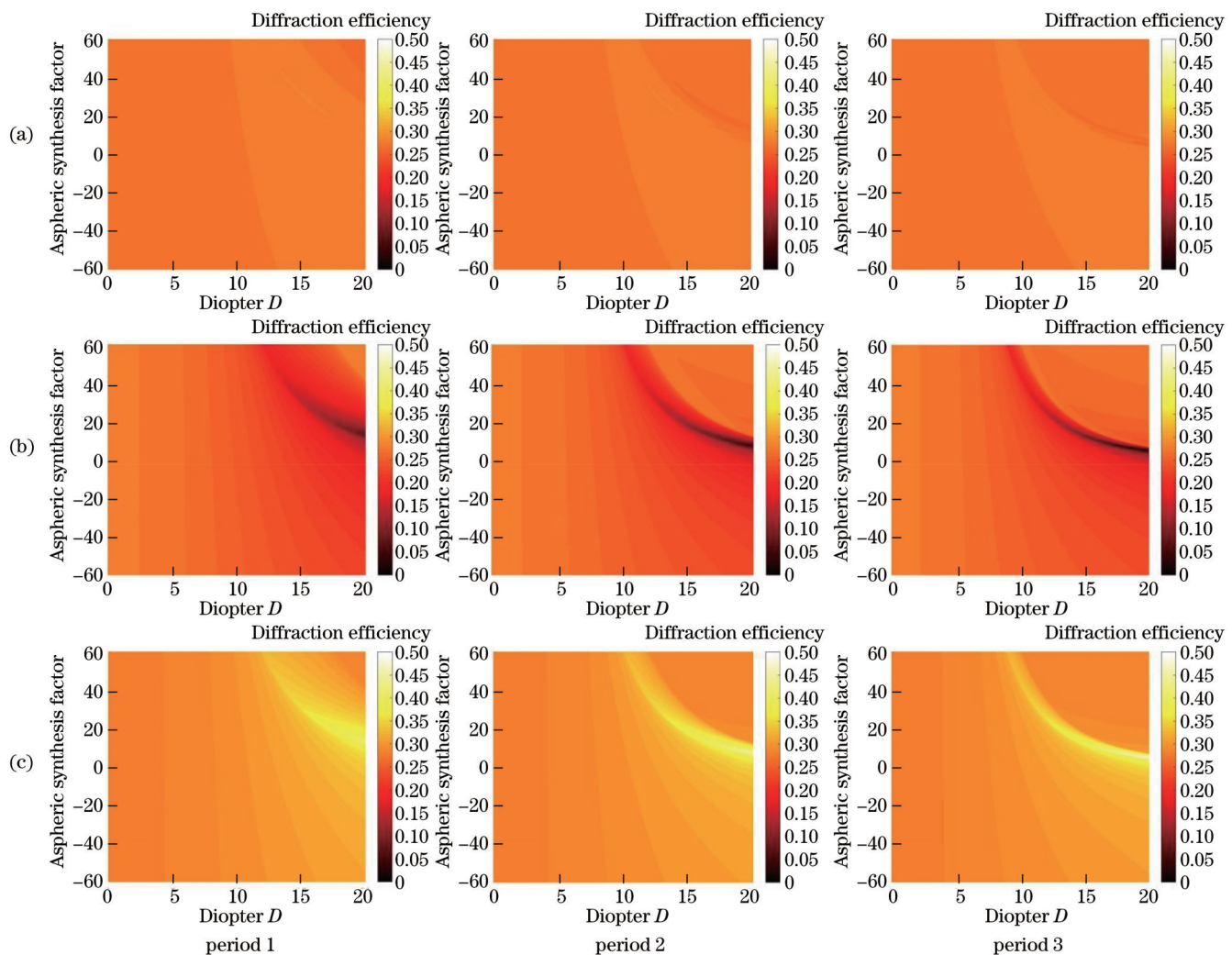


图 6 不同衍射级次下基底屈光度和非球面综合因子对衍射效率的影响分析。(a) $m=0$ ;(b) $m=1$ ;(c) $m=2$

Fig. 6 Analysis of effect of substrate diopter and aspheric synthetic factor on diffraction efficiency at different diffraction orders. (a)  $m=0$ ; (b)  $m=1$ ; (c)  $m=2$

的衍射效率则会更加倾向于平面基底时的衍射效率,即非球面综合因子的加入缓和了由于曲率造成的衍射效率影响;当非球面综合因子为正数时,总体会向着更加弯曲发展,这时总体衍射效率与平面基底时的衍射效率差异更大,即非球面综合因子的加入加重了曲率对衍射效率的影响。综上屈光度以及非球面综合因子的加入导致了总体衍射效率与平面基底衍射效率的差异,进而导致了实际与理论的差距,设计时应避免使用如图 6 中对衍射效率影响过大的参数组合。

其次针对一个非球面衍射基底实例构建了 IOL 的优化过程,衍射基底参数可见表 3,衍射相位参数采用图 6 中分析的参数。对于衍射型 IOL 来说,对单个衍射结构的分析是不恰当的,对衍射部分的分析应该是基于整体衍射结构的分析,同样通过式(19),每个衍射环带需矫正的相位延迟是不同的,则假定光均匀地照射在每个衍射环带上,每个环带的能量比例权重可以用其区域大小来划分,得到每个分区域上不同的优化后的平均相位延迟为

$$\left\{ \begin{array}{l} \dot{\beta}_{\text{opt},1} = \sum_{j=1}^N \frac{r_j}{r} \frac{(n' - n) \beta_{\text{design},1}}{\sqrt{n'^2 - n^2 \sin^2 \theta_{u,1}} - n \cos \theta_{v,1}} \\ \dot{\beta}_{\text{opt},2} = \sum_{j=1}^N \frac{r_j}{r} \frac{(n' - n) \beta_{\text{design},2}}{\sqrt{n'^2 - n^2 \sin^2 \theta_{u,2}} - n \cos \theta_{v,2}} \end{array} \right. , \quad (22)$$

式中: $N$ 为总衍射环带数; $r$ 为衍射结构总环带半径; $\beta_{\text{design},1}$ 、 $\beta_{\text{design},2}$ 为想达到的标准衍射效率时的两区域相位延迟,对于实际衍射效率而言,同样加以权重,得到优化前、后的实际衍射效率表达式为

$$\eta = \sum_{j=1}^N \frac{r_j}{r} c m_j^2 (\lambda_{\text{act}}) . \quad (23)$$

图 7 给出了优化前、优化后的实际衍射效率以及理想衍射效率对比,理论衍射效率由式(6)、式(7)得到,实际衍射效率、优化后实际衍射效率由式(23)得到。如图 7 所示,实际衍射效率偏离理论衍射效率显著,导致了实际应用与理论之间的差距,经过优化后的实际衍射效率曲线几乎与理论衍射效率曲线重合,避

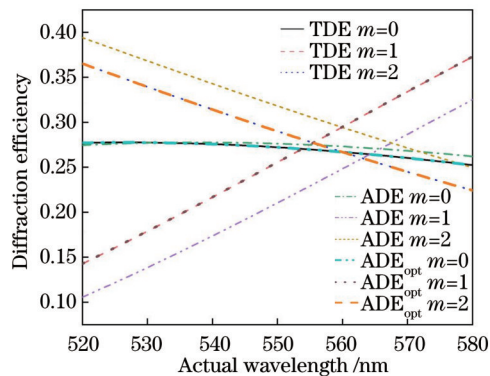


图7 理论衍射效率(TDE)、实际衍射效率(ADE)、优化后实际衍射效率( $ADE_{opt}$ )对比图

Fig. 7 Comparison of theoretical diffraction efficiency (TDE), actual diffraction efficiency (ADE), and optimized actual diffraction efficiency ( $ADE_{opt}$ )

免了这一现象带来的影响,即通过对设计相位延迟的优化,使衍射效率得到了优化。综上,本节详细叙述了多焦点IOL的建立过程与基底分析,综合第2节的方法可得到非球面基底下的多焦点衍射IOL的总体分析设计流程。

## 4 结 论

本文对衍射多焦点IOL设计与基底影响进行了研究。分析了多焦点DOE设计理论模型,设计了一个重点面向中距离的多焦点IOL,该IOL在远、中、近三个焦点处的MTF在100 lp/mm处分别达到了0.5528、0.5840、0.5570,衍射效率分别达到了0.2685、0.3597、0.2223,并根据多焦点DOE设计模型,建立了衍射基底参数对衍射效率的影响的理论模型,从基底屈光度以及基底非球面综合因子两方面进行了分析,提出了优化方法。优化实例表明,优化方程可以降低因基底参数造成的对衍射效率的影响。本文实现了高成像质量的多焦点IOL设计与优化,设计思路可用于多焦点IOL等衍射多焦点眼视透镜设计中。

## 参 考 文 献

- [1] 江曼珊, Lin J. T., 周传清, 等. 人工晶状体的像质分析和优化设计[J]. 光学学报, 2009, 29(s1): 393-395.  
Jiang M S, Lin J T, Zhou C Q, et al. Image analysis and optimize of intraocular lens[J]. Acta Optica Sinica, 2009, 29(s1): 393-395.
- [2] 王振东, 刘欢, 陈阳, 等. 基于谐衍射理论的0.40~2.50 μm宽波段光学系统设计[J]. 激光与光电子学进展, 2022, 59(19): 1922002.  
Wang Z D, Liu H, Chen Y, et al. Design of 0.40 ~ 2.50  $\mu$ m wide band optical system based on harmonic diffraction theory [J]. Laser & Optoelectronics Progress, 2022, 59(19): 1922002.
- [3] 邵加强, 苏宙平. 基于机器学习设计连续相位分布的衍射光学元件[J]. 光学学报, 2023, 43(3): 0323001.  
Shao J Q, Su Z P. Design of diffractive optical elements with continuous phase distribution based on machine learning[J]. Acta Optica Sinica, 2023, 43(3): 0323001.
- [4] Kim G, Dominguez-Caballero J A, Menon R. Design and analysis of multi-wavelength diffractive optics[J]. Optics Express, 2012, 20(3): 2814-2823.
- [5] 毛珊, 赵建林. 镀有增透膜的多层衍射光学元件的优化设计方法[J]. 光学学报, 2019, 39(3): 0305001.  
Mao S, Zhao J L. Optimal design for multi-layer diffractive optical elements with antireflection films[J]. Acta Optica Sinica, 2019, 39(3): 0305001.
- [6] 薛常喜. 多层衍射光学元件成像特性的研究[D]. 长春: 长春理工大学, 2010: 46-49.  
Xue C X, Studies on imaging characteristics of multilayer diffractive optical elements[D]. Changchun: Changchun University of Science and Technology, 2010: 46-49.
- [7] Lin M Y, Chuang C H, Chou T A, et al. A theoretical framework for general design of two-materials composed diffractive Fresnel lens[J]. Scientific Reports, 2021, 11: 15466.
- [8] 张博, 崔庆丰, 薛常喜, 等. 负折射率材料透镜的消色差[J]. 光子学报, 2015, 44(3): 0312004.  
Zhang B, Cui Q F, Xue C X, et al. Achromatism about negative refractive index lens[J]. Acta Photonica Sinica, 2015, 44(3): 0312004.
- [9] 冀畅畅, 刘鑫, 范斌, 等. 基于RGB三波段的消色差衍射透镜设计与分析[J]. 光学学报, 2021, 41(11): 1105001.  
Gong C C, Liu X, Fan B, et al. Design and analysis of diffractive achromats based on RGB three-band[J]. Acta Optica Sinica, 2021, 41(11): 1105001.
- [10] Zeng L, Fang F Z. Advances and challenges of intraocular lens design[J]. Applied Optics, 2018, 57(25): 7363-7376.
- [11] Larsson M, Beckman C, Nyström A, et al. Optical properties of diffractive, bifocal, intraocular lenses[J]. Applied Optics, 1992, 31(13): 2377-2384.
- [12] Loicq J, Willet N, Gatinel D. Topography and longitudinal chromatic aberration characterizations of refractive - diffractive multifocal intraocular lenses[J]. Journal of Cataract and Refractive Surgery, 2019, 45(11): 1650-1659.
- [13] Breyer D R H, Beckers L, Ax T, et al. Aktuelle übersicht: multifokale Linsen und extended-depth-of-focus-intraokularlinsen [J]. Klinische Monatsblätter Für Augenheilkunde, 2020, 237(8): 943-957.
- [14] Davison J A, Simpson M J. History and development of the apodized diffractive intraocular lens[J]. Journal of Cataract & Refractive Surgery, 2006, 32(5): 849-858.
- [15] Cochener B, Boutillier G, Lamard M, et al. A comparative evaluation of a new generation of diffractive trifocal and extended depth of focus intraocular lenses[J]. Journal of Cataract and Refractive Surgery, 2018, 34(8): 507-514.
- [16] Vega F, Alba-Bueno F, Millan M S. Energy efficiency of a new trifocal intraocular lens[J]. Journal of the European Optical Society, 2014, 9: 14002.
- [17] Alio J L, Plaza-Puche A B, Fernández-Buenaga R, et al. Multifocal intraocular lenses: an overview[J]. Survey of Ophthalmology, 2017, 62(5): 611-634.
- [18] Millán M S, Vega F. Extended depth of focus intraocular lens. Chromatic performance[J]. Biomedical Optics Express, 2017, 8 (9): 4294-4309.
- [19] Doskolovich L L, Skidanov R V, Bezus E A, et al. Design of diffractive lenses operating at several wavelengths[J]. Optics Express, 2020, 28(8): 11705-11720.
- [20] Doskolovich L L, Bezus E A, Morozov A A, et al. Multifocal diffractive lens generating several fixed foci at different design wavelengths[J]. Optics Express, 2018, 26(4): 4698-4709.
- [21] Hayashi K, Manabe S I, Hayashi H. Visual acuity from far to near and contrast sensitivity in eyes with a diffractive multifocal intraocular lens with a low addition power[J]. Journal of Cataract & Refractive Surgery, 2009, 35(12): 2070-2076.
- [22] Schiwegerling J. Diffraction efficiency and aberrations of diffractive elements obtained from orthogonal expansion of the point spread function[J]. Proceedings of SPIE, 2016, 9953:

995307.

- [23] 王翼昂, 胡洋, 朴明旭, 等. 含单层衍射元件的可见宽波段计算成像系统设计[J]. 光学学报, 2023, 43(5): 0522001.  
Wang Y A, Hu Y, Piao M X, et al. Design of visible broadband computational imaging system with single-layer diffractive element[J]. Acta Optica Sinica, 2023, 43(5): 0522001.
- [24] 胡洋, 崔庆丰, 孙林, 等. 红外双波段折衍混合光学-数字联合系统设计[J]. 光学学报, 2020, 40(14): 1422002.  
Hu Y, Cui Q F, Sun L, et al. Optical-digital joint design of a dual-waveband infrared refractive-diffractive system[J]. Acta Optica Sinica, 2020, 40(14): 1422002.
- [25] 张博, 崔庆丰, 朴明旭, 等. 双波段多层衍射光学元件的基底材料选择方法研究及其在变焦系统中的应用[J]. 光学学报, 2020, 40(6): 0605001.  
Zhang B, Cui Q F, Piao M X, et al. Substrate material selection method for dual-band multilayer diffractive optical elements and its application in the zoom system[J]. Acta Optica Sinica, 2020, 40(6): 0605001.
- [26] Hazra L N, Delisle C A. Primary aberrations of a thin lens with different object and image space media[J]. Journal of the Optical Society of America A, 1998, 15(4): 945-953.
- [27] Chassagne B, Canioni L. Analytical solution of a personalized intraocular lens design for the correction of spherical aberration and coma of a pseudophakic eye[J]. Biomedical Optics Express, 2020, 11(2): 850-866.
- [28] Zhang A Z. Multifocal diffractive lens design in ophthalmology [J]. Applied Optics, 2020, 59(31): 9807-9823.
- [29] Montagud-Martínez D, Ferrando V, Monsoriu J A, et al. Proposal of a new diffractive corneal inlay to improve near vision in a presbyopic eye[J]. Applied Optics, 2020, 59(13): D54-D58.
- [30] 洪昕, S·J·万诺, 张晓啸. 具有面积不同的衍射区的伪调节眼内透镜: CN101416096B[P]. 2010-11-17.  
Hong X, Vanno S J, Zhang X X. Adjustable intraocular lenses with different size diffraction regions: CN101416096B[P]. 2010-11-17.
- [31] Dong B, Yang Y, Liu Y, et al. Theoretical model and optimization of diffractive optical elements with aspheric substrates in ophthalmology[J]. Applied Optics, 2023, 62(3): 826-835.

## Design and Optimization of Diffractive Multifocal Intraocular Lenses

Dong Bo<sup>1,2</sup>, Yang Ying<sup>1,2</sup>, Xue Changxi<sup>1,2\*</sup>

<sup>1</sup>School of Optoelectronic Engineering, Changchun University of Science and Technology, Changchun 130022, Jilin, China;

<sup>2</sup>Key Laboratory of Advanced Optical System Design and Manufacturing Technology of Universities of Jilin Province, Changchun University of Science and Technology, Changchun 130022, Jilin, China

### Abstract

**Objective** Given the lack of research on the complete design and optimization of multifocal intraocular lenses (IOLs), we propose the design process of diffractive multifocal IOLs focusing on the intermediate distance, and then analyze and optimize the effect of substrate parameters on diffraction efficiency. Multifocal IOLs are mostly based on the superposition of different diffractive optical elements (DOEs) design from inside to outside. When human eyes are in a bright environment, the pupil is relatively small and the edge diffraction periods may not be involved in imaging. Meanwhile, the imaging changes in the transition region and the light interference in adjacent focal points lead to deteriorated visual quality. Thus the multifocal design method with pupil size independent into the IOL optical design becomes a research hotspot, on which many scholars have conducted research. Additionally, as the common view distance of human eyes is intermediate in daily life, optimization of the intermediate distance in multifocal IOL design has also become the focus. On the other hand, DOEs in IOL systems are usually designed with large curvature substrates to carry more diopters due to design space limitations. Combined with the softer material, the diffractive structure is mostly tilted and inclined to be perpendicular to the large curvature substrates, and then the effect of the substrates cannot be ignored. With the continuously improving requirements for visual quality, the future design of IOL substrates will certainly be more inclined to aspheric substrate as a method to improve image quality. In this way, the analysis and optimization of the effect of aspheric substrate parameters on the diffraction performance can bridge the gap between theory and practice in ophthalmic lens design. Through theoretical modeling and simulation analysis, we put forward the analysis and solutions in the above two aspects and hope that our study could serve as a model for the design of diffractive ophthalmic lenses such as multifocal IOLs.

**Methods** On one hand, for the diffractive multifocal IOL design, we analyze the multifocal diffraction efficiency model through diffraction phase changes based on the scalar diffraction theory. Then we build a design model of multifocal IOL based on the Liou-Brennan human eye model through optical software and simultaneously optimize the modulation transfer functions (MTFs) at near, intermediate, and far distances. Generally, the complete design process of diffractive multifocal IOLs is established through the study of diffraction efficiency and MTF optimization. On the other hand, for the case

where the diffractive structure is often tilted and perpendicular to the substrates in IOL design, the schematic design of diffractive IOLs with aspheric substrates is established. By the relationship in the schematic, we derive the expression of period radius and actual phase delay for diffractive IOLs with aspheric substrates. Furthermore, the expression of the actual diffraction efficiency is given for our built multifocal phase profile model. For the example parameters of multifocal IOL design, we analyze and compare the differences between the actual diffraction efficiency and the theoretical diffraction efficiency in terms of the diopters and aspheric synthesis factors. Finally, an optimization method is proposed based on assigning corresponding weights to different periods to compensate for the effect on diffraction efficiency.

**Results and Discussions** Firstly, the diffraction efficiency distribution of multifocal DOE is obtained by the theory model of phase profile [Eqs. (6) and (7)], and the relationship between phase delay  $\beta_1$ ,  $\beta_2$ , and diffraction efficiency at each order and overall orders in our experiment is analyzed [Figs. 1(a) and 1(b)]. The diffraction phase profile is obtained according to the focused optimization design of intermediate distance [Fig. 1(c)], and the results show that the diffraction efficiency of the obtained model reaches 0.2685, 0.3597, and 0.2223 at far, intermediate, and near focal points, respectively (Table 1). A multifocal diffraction design focusing on intermediate distance optimization is also obtained. Meanwhile, we establish and optimize a diffractive multifocal IOL system by Zemax, and the MTFs of far, intermediate, and near distances are 0.5528, 0.5840, and 0.5570 at 100 lp/mm, respectively which exceed the MTF of the Liou-Brennan model at 100 lp/mm (Fig. 2) with high imaging quality of IOL design. Then the effect model of diffraction substrate parameters is proposed for the multifocal DOE phase profile design (Fig. 4), and the expressions of ophthalmic lens period radius, actual phase delay, and actual diffraction efficiency for aspheric substrates are obtained. Additionally, analysis of the actual diffraction efficiency can be employed to pick the substrate diopters and aspheric synthesis factors for ideal diffraction efficiency (Fig. 6). We further provide an optimization method, and the results indicate that the optimized diffraction efficiency is in close agreement with the theoretical value and achieves our optimization objective (Fig. 7).

**Conclusions** We conduct the diffractive multifocal IOL design and substrate effect analysis. Firstly, the theoretical model of multifocal DOE design is analyzed, and a multifocal IOL focusing on intermediate distance is designed. The MTFs of the IOL at three focal points of far, intermediate, and near distance are 0.5528, 0.5840, and 0.5570 at 100 lp/mm, and the diffraction efficiency reaches 0.2685, 0.3597, and 0.2223, respectively. Then according to the phase profile of multifocal DOE, a theoretical model of the effect of diffractive substrate parameters on diffraction efficiency is built, and the theoretical model in terms of both substrate diopters and substrate aspheric synthesis factors is analyzed. Finally, we propose an optimization method for the substrate effect, and the optimization example shows that the optimization equation can reduce the influence on diffraction efficiency caused by substrate parameters. The design and optimization of multifocal IOLs with high imaging quality are realized, and the ideas can be applied in designing diffractive multifocal IOLs and other multifocal ophthalmic lenses.

**Key words** diffraction optics; intraocular lens; multi focus; diffraction efficiency